zek00911/zek3773d11z | xppws | S=1 | 7/12/11 | Art: 5066-11
zjs / DOCHEAD=ARTICLE zjss / DOCTOPIC=ARTICLES
FROM COVER SHEET: Editor: Kuspa Article No.: T Section: Articles

EUKARYOTIC CELL, Sept. 2011, p. 000 Vol. 10, No. 9
1535-9778/11/$12.00 doi:10.1128/EC.05066-11

Different Roles of Membrane Potentials in Electrotaxis and Chemotaxis of *Dictyostelium* Cells▽†

Run-Chi Gao,[1,2,3] Xiao-Dong Zhang,[1] Yao-Hui Sun,[1] Yoichiro Kamimura,[3] Alex Mogilner,[4] Peter N. Devreotes,[3] and Min Zhao[1]*

Department of Dermatology and Department of Ophthalmology, Institute for Regenerative Cures, School of Medicine, University of California at Davis, Davis, California 95817[1]; Yunnan Normal University, Kunming, Yunnan, China 650092[2]; Department of Cell Biology and Anatomy, Johns Hopkins University, School of Medicine, MD 21205[3]; and Department of Neurobiology, Physiology and Behavior and Department of Mathematics, University of California at Davis, Davis, California 95616[4]

Received 6 April 2011/Accepted 27 June 2011

Many types of cells migrate directionally in direct current (DC) electric fields (EFs), a phenomenon termed galvanotaxis or electrotaxis. The directional sensing mechanisms responsible for this response to EFs, however, remain unknown. Exposing cells to an EF causes changes in plasma membrane potentials (V_m). Exploiting the ability of *Dictyostelium* cells to tolerate drastic V_m changes, we investigated the role of V_m in electrotaxis and, in parallel, in chemotaxis. We used three independent factors to control V_m: extracellular pH, extracellular [K^+], and electroporation. Changes in V_m were monitored with microelectrode recording techniques. Depolarized V_m was observed under acidic (pH 5.0) and alkaline (pH 9.0) conditions as well as under higher extracellular [K^+] conditions. Electroporation permeabilized the cell membrane and significantly reduced the V_m, which gradually recovered over 40 min. We then recorded the electrotactic behaviors of *Dictyostelium* cells with a defined V_m using these three techniques. The directionality (directedness of electrotaxis) was quantified and compared to that of chemotaxis (chemotactic index). We found that a reduced V_m significantly impaired electrotaxis without significantly affecting random motility or chemotaxis. We conclude that extracellular pH, [K^+], and electroporation all significantly affected electrotaxis, which appeared to be mediated by the changes in V_m. The initial directional sensing mechanisms for electrotaxis therefore differ from those of chemotaxis and may be mediated by changes in resting V_m.

AQ: A

Fn2

Cells migrate directionally in response to many extracellular cues including chemical gradients (chemotaxis), topography, mechanical forces (mechanotaxis/durataxis), and electrical fields (EFs) (electrotaxis/galvanotaxis) (1, 3, 8, 15, 27). Electric fields have long been suggested to be a candidate directional signal for cell migration in development, wound healing, and regeneration. The mechanisms used by cells to sense the weak direct current (DC) EFs, however, have remained very poorly understood.

One of the immediate effects felt by a cell upon exposure to an EF is a change in the cell membrane potentials (V_m). In an EF, the plasma membrane facing the cathode depolarizes while the membrane facing the anode hyperpolarizes (17, 18). It has been proposed that the changes in V_m may underlie electrotaxis. In a cell with negligible voltage-gated conductance, the hyperpolarized membrane facing the anode attracts Ca^{2+} by passive electrochemical diffusion. This side of the cell then contracts, thereby propelling the cell toward the cathode. In a cell with voltage-gated Ca^{2+} channels, channels near the cathodal (depolarized) side open, thereby allowing Ca^{2+} influx. Intracellular Ca^{2+} levels will rise both on the anodal side and on the cathodal side in such a cell. The direction of cell movement in this situation will depend on the balance between the opposing contractile forces (17). The role of V_m in electrotaxis has not yet been directly tested.

In this report, we used *Dictyostelium* cells to test this directly. *Dictyostelium* cells show a robust electrotaxis and tolerate significant changes in V_m while maintaining good motility under conditions of different extracellular pH values and ion concentrations and even following electroporation (20, 25, 29). These features make *Dictyostelium* cells a unique testing model. We quantified electrotaxis and chemotaxis of cells with well-controlled V_ms by varying three independent factors. We found that the V_m indeed regulated electrotaxis while having no effect on chemotaxis. We thus identified a contrasting role of V_m between electrotaxis and chemotaxis which may underlie the mechanisms used by cells to sense weak dc EFs.

AQ: B

MATERIALS AND METHODS

Cell culture and development. *Dictyostelium discoideum* AX3 cells were grown axenically in HL5 medium. Vegetative cells were washed and starved in development buffer (DB) and then were pulsed with 50 nM cyclic AMP (cAMP) every 6 min for an additional 4 h (29). All procedures were carried out at room temperature (~22°C).

Micropipette chemotaxis assay. Chemotaxis experiments were performed as reported (4, 10). Briefly, 20 μl of cells (1×10^5 to 4×10^5 cells/ml) in DB were seeded onto a coverslip chamber. Bathing solutions with different pH values or different K^+ concentrations were then introduced. A Femtotip microinjection needle filled with 10 μM cAMP was placed into the field, and a positive pressure of 25 lb/in^2 was applied via a connected microinjector. Chemotaxis was recorded by time-lapse video using an inverted microscope (CKX41; Olympus) with a 10× objective lens. Images were taken every 30 s for 30 min.

Electrotaxis assay. Electrotaxis experiments were carried out as described previously (21, 28, 29). Developed cells were seeded into an electrotactic chamber. After 10 min of incubation, unattached cells were removed by gently washing

* Corresponding author. Mailing address: 2921 Stockton Blvd., University of California, Sacramento, CA 95817. Phone: (916) 703 9381. Fax: (916) 703 9384. E-mail: minzhao@ucdavis.edu.

† Supplemental material for this article may be found at http://ec.asm.org/.

▽ Published ahead of print on 8 July 2011.

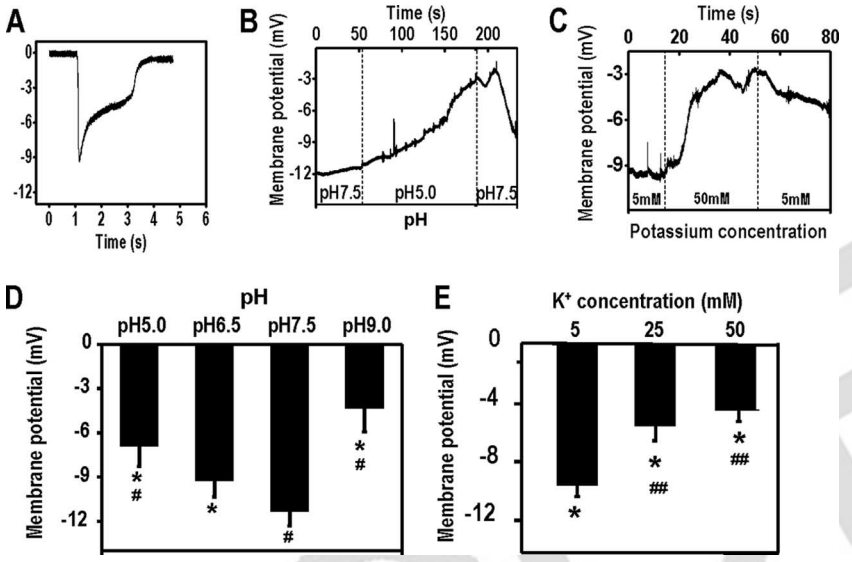

FIG. 1. Extracellular pH and K^+ concentration regulate the membrane potential (V_m) of *Dictyostelium* cells. Developed *Dictyostelium* cells were bathed in DB with different pH values and K^+ concentrations. V_m was measured by microelectrode impalement. (A) Typical peak-shaped potential transient that was recorded upon microelectrode penetration of a *D. discoideum* cell bathed in DB with different pH values or K^+ concentrations. (B and C) Continuous recording of V_m with an extra-fine electrode showed stable stationary V_m of *D. discoideum*. The dotted vertical line indicates the time when the bathing solution was replaced with a buffer of a different pH value or different K^+ concentration. (D) Averaged V_ms from 21 cells (pH 5.0), 16 cells (pH 6.5), 16 cells (pH 7.5), and 16 cells (pH 9.0). *, $P < 0.001$ compared to that in pH 7.5; #, $P < 0.001$ compared to that in pH 6.5. (E) Averaged V_ms from 13 cells (5 mM K^+), 16 cells (25 mM K^+), and 24 cells (50 mM K^+). *, $P < 0.001$ compared to that in buffer with K^+ concentration of 0.5 mM K^+; #, $P < 0.001$ compared to that in K^+ concentration of 5 mM K^+.

with DB. Cells were then bathed in defined buffers, as indicated, with different pH values or different K^+ concentrations in parallel with the chemotaxis assay. For cells treated with electroporation, normal DB (pH 6.5, 5 mM K^+) was used, and the EF was switched on 10 min after seeding.

The applied EF was maintained at 12 V/cm for 30 min. Time-lapse images of cell migration were acquired using an inverted microscope (Axiovert 40; Carl Zeiss) equipped with a charge-coupled-device (CCD) camera (C4742-95; Hamamatsu Corporation) and a motorized XYZ stage (BioPoint 2; Ludl Electronic Products, Ltd.), and controlled by Simple PCI, version 5.3, imaging software.

Quantitative analysis of electrotaxis and chemotaxis. Chemotaxis and electrotaxis were analyzed as previously described (4, 29). The chemotactic index and electrotactic index were used to quantify how, directionally, cells migrated toward cAMP or in response to an EF, respectively. To calculate the chemotactic index or electrotactic index, the cosine of the angle between the direction of movement and the direction of the chemoattractant gradient or electric vector was determined (29). For migration speed, we used trajectory and displacement speeds (29). Persistency was further calculated as the shortest linear distance between the start and endpoints of the migration path divided by the total distance traveled by a cell. All motile isolated cells were analyzed. At least 30 cells from three independent experiments were analyzed.

Membrane potential (V_m) measurements. Cells were seeded on a sterile glass coverslip and observed with a 60× objective. V_m measurements were conducted using fine-tipped glass pipette microelectrodes. Two types of recording, transient and continuous, were used to verify each other. The pipettes were pulled from borosilicate glass (World Precision Instruments, Sarasota, FL) using a PP-830 pipette puller (Narishige International, Inc., New York, NY), and the resistance was ~20 MΩ when the pipettes were filled with 3 M KCl solution, as measured in the DB. Recordings were performed using a GeneClamp 500 amplifier (Axon Instrument/Molecular Devices, Union City, CA). The signals were digitally filtered at 1 kHz and digitized at 2 kHz using a Digidata 1322A digitizer and pClamp, version 9.0, software (Axon Instrument/Molecular Devices).

DB solution was used as the standard recording solution. The solutions with higher or lower pH values were obtained by adding HCl or NaOH. The solutions with different K^+ concentrations were made by using 3 M KCl and normal DB. All experiments were conducted at room temperature, and the recording was repeated in 16 or more cells.

Our measurements (both transient impalement and continuous recording) showed similar V_m values, which were consistent with other published recordings (24).

Modulation of membrane potential (V_m). The first method used to control V_m was to maintain cells in four bathing solutions with pH values of 5.0, 6.5, 7.5, and 9.0. All solutions were autoclaved and stored at room temperature until use. Before measurement of V_m or chemotaxis and electrotaxis experiments, cells were bathed in a defined solution for ~10 min. The second method modulated V_m by adjusting the recording buffer [K^+] at three concentrations (5 mM, 25 mM, and 50 mM). The K^+ concentrations were verified with an ion-selective probe. All solutions were autoclaved. The third method was electroporation, which was carried out as previously described (7, 11). Electroporation was performed in a Gene Pulser Xcell Electroporation System (Bio-Rad) with two pulses of 0.85 kV/25 μF with a resistance-capacitance (RC) time of 1 ms, separated by a 5-s interval. For V_m measurements, 20 μl of cell suspension was immediately taken out of the electroporation chamber and placed in a petri dish in DB and measured 10 min later.

Statistics. Pearson's correlation coefficient and a chi-square test were performed when pertinent. All data points were presented as means ± standard errors of the means (SEM) averaged from at least three measurements.

RESULTS

Extracellular pH and K^+ concentration regulated V_m in *Dictyostelium* cells. A typical negative peak potential was transiently observed upon impalement of a *Dictyostelium* cell with a microelectrode. V_m transiently reached a peak value within several milliseconds of impalement; the potential quickly decreased due to leakage (Fig. 1A). The initial peak value was used to reflect the V_m, as in previous studies (24, 25). The values were verified with the continuous measurement. We achieved continuous recording using microelectrodes with an extremely fine tip (resistance up to 30 MΩ) that penetrates a cell so the V_m can be reliably monitored continuously for a

zek00911/zek3773d11z | xppws | S=1 | 7/12/11 | Art: 5066-11

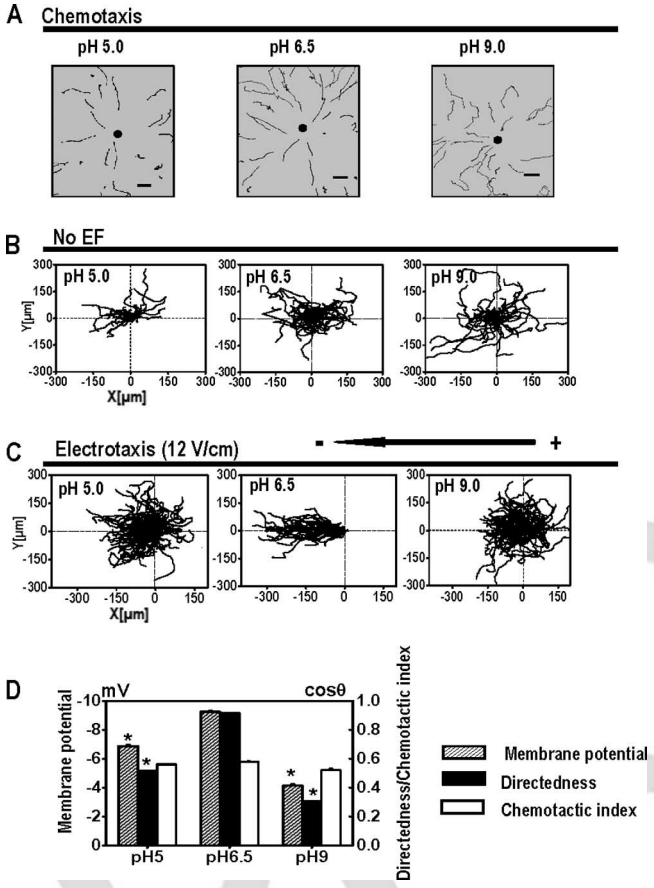

FIG. 2. Extracellular pH plays different roles in chemotaxis and electrotaxis in *Dictyostelium* cells. (A) cAMP gradients were formed from the tip of a micropipette filled with 10 μM cAMP. Trajectories of cell migration toward cAMP in DB with different pH values are indicated. Dark spots represent the position of the micropipette. Scale bar, 20 μm. (B) Cell migration in random directions under control conditions without an EF although cells were bathed in DB with different pH values as indicated. (C) Cell migration trajectories in which the start point of each cell is set as the origin. Cells migrated cathodally in a pH of 6.5 in an EF. However, directed cell migration was significantly impaired under acidic (pH 5.0) or alkaline (pH 9.0) conditions. (D) The effects of extracellular pH on electrotaxis in *Dictyostelium* cells correlate with the effects on V_m. *Dictyostelium* cells bathed in pH 6.5 showed a greater V_m than that of the cells in pH 5.0 or pH 9.0 and significantly better electrotaxis. The changes in pH and corresponding changes in V_m did not significantly affect the chemotaxis (chemotactic index). *, $P < 0.001$ compared to that in pH 6.5.

much longer time, usually several minutes in contrast to milliseconds in the first method (Fig. 1B and C). AQ: F

We first quantified the effect of extracellular pH and $[K^+]$ on V_m. Being bathed in solutions of different pH values and K^+ concentrations resulted in significant and consistent changes in V_m (Fig. 1). An example of continuous recording of the dynamic change in V_m, in which extracellular pH dropped from 7.5 to 5.0 and then went back up to 7.5, showed that the V_m remained stable and was responsive to pH changes over several minutes (Fig. 1B). The membrane significantly depolarized when the pH either dropped to 5.5 or increased to 9.0 (Fig. 1D). The maximal V_ms were recorded at pH 7.5 and 5 mM K^+.

Chemotaxis and electrotaxis in bathing solutions with different pH values. To test the effects of depolarizing V_m on chemotaxis, we used a needle chemotaxis assay and quantitatively analyzed the directional cell migration. Without cAMP gradient, cells bathed in different solutions showed similar patterns of migration in random directions. In buffer solutions of pH 5.0, pH 6.5, and pH 9.0, no significant differences in cell morphology, behavior, or trajectory speed were observed among cells in response to the cAMP gradient (Fig. 2A and D; Table 1). This is consistent with a previous report (25). F2 T1/AQ:G

The electrotaxis of *Dictyostelium* cells, however, is significantly altered by the pH of the bathing solution. The chemotactic indexes for cells bathed in DB of pH 5.0, pH 6.5, and pH 9.0 were 0.56 ± 0.01, 0.58 ± 0.01, and 0.52 ± 0.01, respectively. However, electrotaxis was significantly affected by bathing solution pH (Fig. 2C and D). Cells in solutions of pH 6.5 had more negative V_ms and showed the best electrotaxis. Cells in pH 5.0 or pH 9.0 showed significantly reduced electrotaxis, with directedness values of 0.51 ± 0.01 or 0.30 ± 0.01, respectively (Fig. 2D).

Chemotaxis and electrotaxis of K^+-induced depolarized *Dictyostelium* cells. We then examined the effect of extracellular $[K^+]$ on chemotaxis and electrotaxis. Cells bathed in buffer of 5 mM K^+ moved toward cAMP with a typically polarized morphology. In buffer of 50 mM K^+, cells near the micropipette tip moved toward the cAMP source. Cells further away from the tip appeared to move less directionally toward the pipette. Nonetheless, directional migration was evident (Fig. 3A). Cells in 50 mM K^+ migrated with a reduced chemotactic index of 0.30 ± 0.01, compared to that of 0.58 ± 0.01 for cells in 5 mM K^+ (Fig. 3D). F3

Extracellular $[K^+]$ significantly affected electrotaxis. Cells bathed in buffer with 5 mM K^+ showed robust electrotaxis with a directedness value of 0.93 ± 0.01 (Fig. 3D). The directedness gradually decreased to 0.64 in 25 mM K^+ and 0.24 in 50 mM K^+ (Fig. 3D). Cells bathed in buffer with 50 mM K^+ had a significantly lower directedness value, representing a decrease of 73%. Although increasing extracellular $[K^+]$ appeared to inhibit both chemotaxis and electrotaxis, it seemed to have a more significant effect on electrotaxis (Table 2). T2/AQ:H

Electroporation depolarized V_m and abolished electrotaxis. To further verify the role of V_m in electrotaxis, we used electroporation to depolarize *Dictyostelium* cells. Electroporation with high-voltage pulses permeabilizes the cell plasma membrane, thus significantly depolarizing V_m by causing a large increase in non-ion-selective membrane permeability. Measurements in electroporated cells showed that the membrane is

TABLE 1. The effects of extracellular pH and K^+ on chemotaxis[a]

Developing buffer	Trajectory speed (μm/min)	Displacement speed (μm/min)	Chemotactic index	Persistency
pH 5.0	4.69 ± 0.03	3.34 ± 0.03	0.56 ± 0.01	0.79 ± 0.01†
pH 6.5	5.01 ± 0.02	3.06 ± 0.02	0.58 ± 0.01	0.70 ± 0.01
pH 9.0	3.89 ± 0.02‡	2.07 ± 0.02†	0.52 ± 0.01	0.64 ± 0.01
5 mM K^+	5.01 ± 0.02	3.06 ± 0.02	0.58 ± 0.01	0.70 ± 0.01
50 mM K^+	4.26 ± 0.03	1.62 ± 0.03*	0.30 ± 0.01*	0.65 ± 0.01

[a] The data represent means ± SEM. *, $P < 0.001$, compared to buffer using 5 mM K^+; †, $P < 0.01$, compared to buffer at buffer at pH 6.5; ‡, $P < 0.001$, compared to buffer at buffer at pH 6.5.

zek00911/zek3773d11z | xppws | S=1 | 7/12/11 | Art: 5066-11

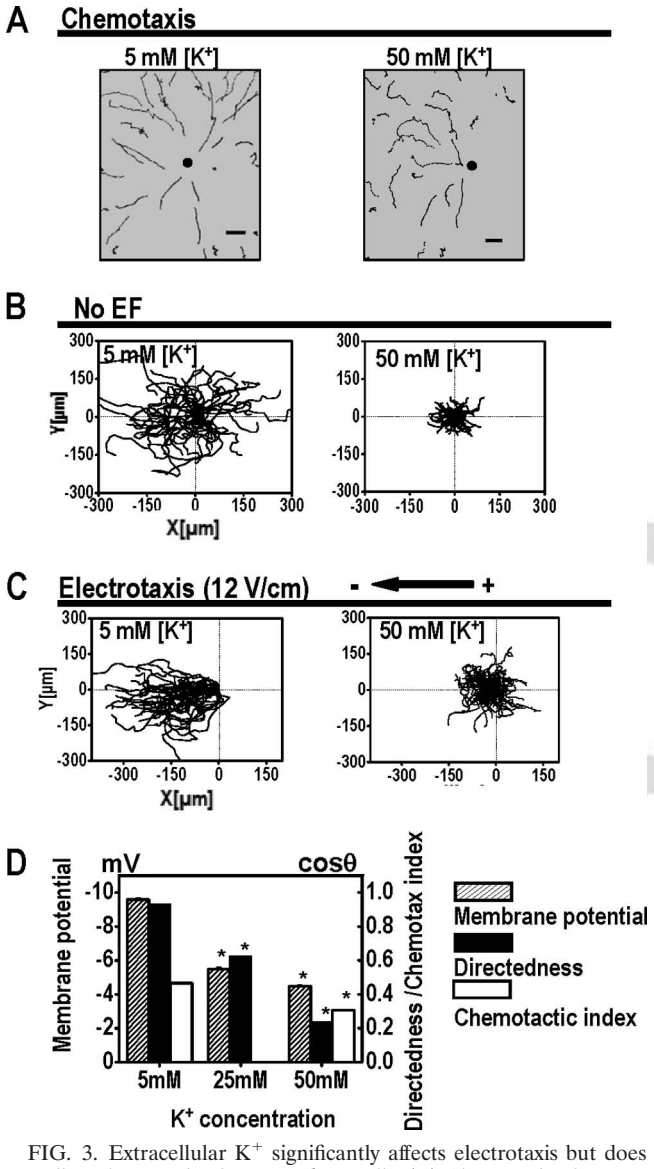

FIG. 3. Extracellular K^+ significantly affects electrotaxis but does not affect chemotaxis of *Dictyostelium* cells. (A) Chemotaxis of *Dictyostelium* cells in buffer with different extracellular K^+ concentrations. Cells in buffer with 5 mM or 50 mM K^+ were able to undergo chemotaxis. Trajectories show that cells migrate toward cAMP. Dark spots represent the positions of micropipette tips. Scale bar, 20 μm. (B) Cells migrate in random directions in buffer with 5 mM or 50 mM K^+ without an applied EF. (C) Cells migrate cathodally in DB with 5 mM and 50 mM K^+. When the K^+ concentration increased V_m decreased) (Fig. 1), and electrotaxis was significantly reduced. (D) The effects of extracellular K^+ on electrotaxis in *Dictyostelium* cells correlated with the effects on V_m. Cells in buffer with 50 mM K^+ had a significantly reduced V_m as well as significantly reduced electrotaxis. Slightly reduced chemotactic activity was seen with higher concentrations of K^+ solution. AQ: M

significantly depolarized following electroporation. In the data shown in Fig. 4, the starting time (0 min) was set as the time of electroporation. All cells measured at 10 min following electroporation showed a significantly reduced V_m, which recovered gradually. The recovery took roughly 30 to 40 min following electroporation (Fig. 4A). F4

Electrotaxis in electroporation-induced depolarized cells was lost. Batch-matched control cells had good directional migration with a directedness value of 0.96 ± 0.01 within 10 min in an EF, which was maintained through 20 to 30 min (Fig. 4C). Following electroporation, electrotaxis was completely inhibited (Fig. 4B). In the first 20 min following electroporation, the directedness of cells in an EF was almost zero. At 30 to 40 min, some directedness reappeared as V_m recovered to a certain degree (Fig. 4D).

We analyzed the relationship between these parameters and V_m. We found that V_m correlates significantly well with electrotaxis, with a correlation coefficient of −0.77 (Fig. 5A), whereas chemotaxis did not appear to correlate with the changes in V_m (Fig. 5B). F5

DISCUSSION

We tested the effects of extracellular pH and $[K^+]$ on electrotaxis using *Dictyostelium* cells, which have the unique property of tolerating changes in extracellular pH, $[K^+]$, and even electroporation, while maintaining good motility. We found that (i) changes in extracellular pH and $[K^+]$ and electroporation significantly affected V_m and that (ii) reduced V_m in response to these three factors significantly inhibited electrotaxis. The inhibitory effect on electrotaxis correlated well with the reduced V_m, but chemotactic effects did not. AQ: I

In developed *Dictyostelium* cells, cAMP binds G protein-coupled receptors, activates $G\alpha2\beta\gamma$, small GTPase, and class 1 phosphatidylinositol-3 kinases (PI3K), thereby phosphorylating phosphatidylinositol-3,4-bisphosphate $[PI(3,4)P_2]$ into phosphatidylinositol-3,4,5-trisphosphate $[PI(3,4,5)P_3]$, and finally induces F-actin polymerization, resulting in pseudopod development. Several other pathways may also contribute to chemotaxis (9, 22). We demonstrated that *Dictyostelium* cells also show robust electrotaxis and are a good model for dissecting the molecular/genetic basis of electrotaxis (19, 29).

Extracellular pH, $[K^+]$, and electroporation significantly affected V_m and correspondingly reduced or abolished electrotaxis. When V_m recovered, electrotaxis was restored. V_m in *Dictyostelium* cells is mainly generated by electrogenic proton pumps (24, 25). By varying extracellular pH, we controlled the V_m with good reproducibility. The V_m values were smaller than those reported previously (24, 25). We used two different recording methods to confirm the measurements. The difference in V_m values may be due to other modifications: (i) the AX3 strain was used here whereas NC4 was used before; (ii) we

TABLE 2. The effects of pH and K^+ on electrotaxis[a]

Developing buffer	Trajectory speed (μm/min)	Displacement speed (μm/min)	Directedness	Persistency
pH 5.0	9.27 ± 0.02*†	4.79 ± 0.02*†	0.51 ± 0.01*†	0.52 ± 0.01*†
pH 6.5	14.79 ± 0.08*	10.75 ± 0.07*	0.95 ± 0.01	0.73 ± 0.02
pH 7.5	11.68 ± 0.06†	9.20 ± 0.06†	0.97 ± 0.01	0.78 ± 0.01
pH 9.0	9.05 ± 0.02*†	4.42 ± 0.02*†	0.30 ± 0.01*†	0.50 ± 0.01*†
5 mM K^+	13.09 ± 0.05	8.55 ± 0.04	0.93 ± 0.01	0.66 ± 0.01
25 mM K^+	6.15 ± 0.03‡	3.57 ± 0.02‡	0.64 ± 0.01‡	0.59 ± 0.01
50 mM K^+	6.46 ± 0.01‡	2.95 ± 0.01‡	0.24 ± 0.01‡	0.46 ± 0.00‡

[a] The data represent means ± SEM. *, $P < 0.001$ compared to buffer at pH 7.5; †, $P < 0.001$ compared to buffer pH 6.5; ‡, $P < 0.001$ compared to that in buffer with 5 mM K^+.

zek00911/zek3773d11z | xppws | S=1 | 7/12/11 | Art: 5066-11

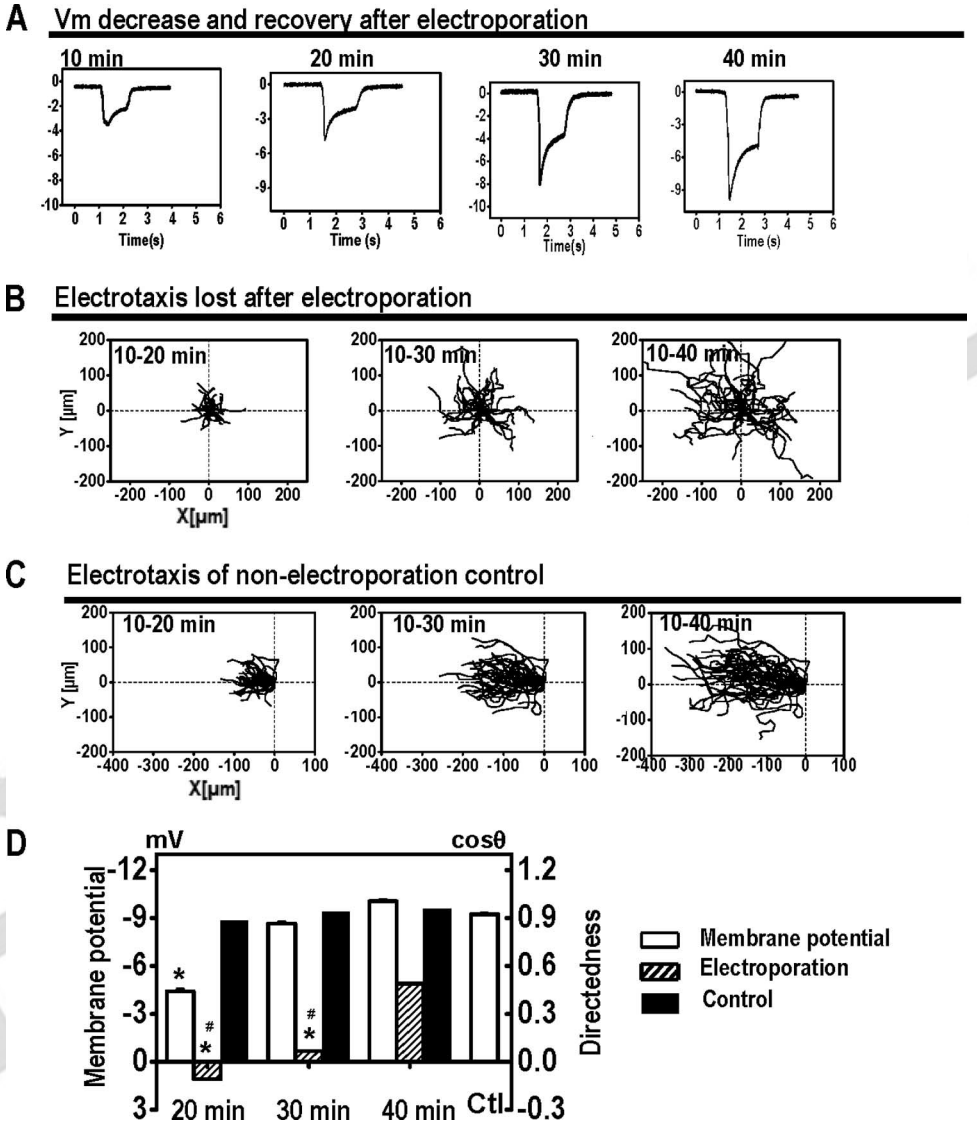

FIG. 4. Electroporation depolarizes membrane potential (V_m) and abolishes electrotaxis. (A) Representative V_m measured at pH 6.5 after electroporation. The moment of electroporation was set as time zero. (B) Electroporated cells lost the electrotactic response, which showed some degree of recovery 30 min later (see video S6 in the supplemental material). (C) Control cells showed robust electrotaxis. (D) Loss of electrotaxis correlated well with V_m. When V_m recovered, electrotaxis recovered significantly. Control, V_m in control cells not electroporated. The EF was 12 V/cm. *, $P < 0.001$ compared to that of cells not being electroporated; #, $P < 0.001$ compared to that of cells after 40 min of recovery following electroporation.

used DB buffer while Van Duijn and coworkers used a Na^+-saline (40 mM NaCl, 5 mM KCl, 1 mM $CaCl_2$ and 5 mM HEPES-NaOH, pH 7.0); (iii) we used different development protocols (24, 25). The concentration of extracellular K^+ affects V_m (26). Different extracellular K^+ concentrations regulated V_m: the higher the K^+ concentration, the lower the V_m (Fig. 1).

AQ: J

At 50 mM K^+, electrotaxis was significantly inhibited (Fig. 3). Depolarization of cells following electroporation abolished the electrotactic response while recovery of V_m restored the electrotactic response (Fig. 4). Chemotaxis of the cells with an altered V_m, modulated by changes in extracellular pH or [K^+], was largely unaffected. This is consistent with a previous report (25). Collectively, these results support the theory that the inhibition of electrotaxis by changes in extracellular pH, [K^+], and electroporation appears to be a specific effect caused by changes to V_m. The genome of *Dictyostelium* cells shows at least two possible transient receptor potential (TRP) channel genes, a Ca^{2+} channel gene, and several K^+ channel genes (14). Several signal transduction pathways related to electrotaxis could depend on V_m caused by the interactions between ion channels and other signaling proteins such as integrins (2, 5, 6, 12, 13, 16, 23). It may involve different membrane proteins, such as ion channels, transporters, receptors, and the actin cytoskeleton, and may also involve Ca^{2+} signaling (20). The reduced V_m might inhibit Ca^{2+} signaling and thereby affect electrotaxis. Another possibility is that V_m may control the sensors that detect the EFs. We are currently using a

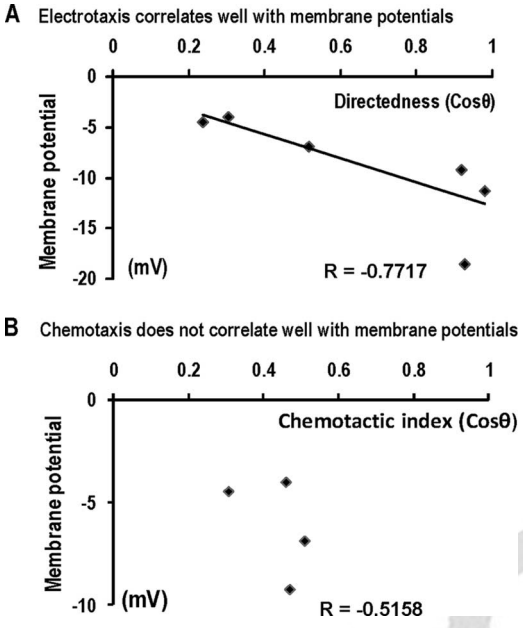

FIG. 5. Significant correlation is between V_m and electrotaxis but not chemotaxis. (A) Scatter plot shows electrotactic directedness and resting membrane potential ($r = -0.77$). The best-fit line is shown. (B) Scatter plot shows chemotactic index and membrane potential ($r = -0.51$).

high-throughput strategy to screen for such sensing molecules in electrotaxis.

In conclusion, changes in extracellular pH, $[K^+]$, and electroporation all had significant effects on electrotaxis. When the V_m was depolarized, electrotaxis was significantly inhibited. Extracellular pH, $[K^+]$, and electroporation all had significant effects on electrotaxis, which appeared to be mediated by the changes in V_m. The initial directional sensing mechanisms for electrotaxis therefore differ from those in chemotaxis and may be mediated by changes in V_m.

ACKNOWLEDGMENTS

This work was supported by a grant from the NSF (MCB-0951199 to M.Z. and P.N.D.). M.Z. is also supported by NIH grant 1R01EY019101, California Institute of Regenerative Medicine grant RB1-01417, and the University of California at Davis (UC Davis) Dermatology Developmental Fund. This study was supported in part by an unrestricted grant from Research to Prevent Blindness, UC Davis Ophthalmology, and Yunnan Province Talented Recruiting Program (2009CI127). We thank the Wellcome Trust for continuous support (WT082887MA to M.Z.).

We thank Lin Cao and Kristen Swaney for sharing technical expertise and other members of the Zhao and Devreotes laboratories for their help. We thank Tsung-Yu Chen for kindly providing the electrophysiological equipment and Liping Nie for kindly helping us to use her electroporation device.

M.Z., P.N.D., A.M., X.-D.Z., and R.C.-G. designed the research; R.C.-G., X.-D.Z., Y.-H.S., and Y.K. performed research; M.Z., R.C.-G., X.-D.Z., and Y.-H.S. analyzed data; R.C.-G., X.-D.Z., and M.Z. wrote the paper with help from Y.-H.S.

We declare that we have no conflicts of interest.

REFERENCES

1. **Barreiro, O., P. Martin, R. Gonzalez-Amaro, and F. Sanchez-Madrid.** 2010. Molecular cues guiding inflammatory responses. Cardiovasc. Res. **86:**174–182.
2. **Becchetti, A., S. Pillozzi, R. Morini, E. Nesti, and A. Arcangeli.** 2010. New insights into the regulation of ion channels by integrins. Int. Rev. Cell Mol. Biol. **279:**135–190.
3. **Berzat, A., and A. Hall.** 2010. Cellular responses to extracellular guidance cues. EMBO J. **29:**2734–2745.
4. **Cai, H., et al.** 2010. Ras-mediated activation of the TORC2-PKB pathway is critical for chemotaxis. J. Cell Biol. **190:**233–245.
5. **Dai, S., D. D. Hall, and J. W. Hell.** 2009. Supramolecular assemblies and localized regulation of voltage-gated ion channels. Physiol. Rev. **89:**411–452.
6. **Davis, M. J., et al.** 2002. Regulation of ion channels by integrins. Cell Biochem. Biophys. **36:**41–66.
7. **Gaudet, P., K. E. Pilcher, P. Fey, and R. L. Chisholm.** 2007. Transformation of *Dictyostelium discoideum* with plasmid DNA. Nat. Protoc. **2:**1317–1324.
8. **Goetz, J. G.** 2009. Bidirectional control of the inner dynamics of focal adhesions promotes cell migration. Cell Adh. Migr. **3:**185–190.
9. **Insall, R. H.** 2010. Understanding eukaryotic chemotaxis: a pseudopod-centred view. Nat. Rev. Mol. Cell Biol. **11:**453–458.
10. **Kamimura, Y., M. Tang, and P. Devreotes.** 2009. Assays for chemotaxis and chemoattractant-stimulated TorC2 activation and PKB substrate phosphorylation in *Dictyostelium*. Methods Mol. Biol. **571:**255–270.
11. **Knecht, D., and K. M. Pang.** 1995. Electroporation of *Dictyostelium discoideum*. Methods Mol. Biol. **47:**321–330.
12. **Liang, W., et al.** 2010. Role of phosphoinositide 3-kinase α, protein kinase C, and L-type $Ca2^+$ channels in mediating the complex actions of angiotensin II on mouse cardiac contractility. Hypertension **56:**422–429.
13. **Liu, B., et al.** 2009. Enhancement of BK(Ca) channel activity induced by hydrogen peroxide: involvement of lipid phosphatase activity of PTEN. Biochim. Biophys. Acta **1788:**2174–2182.
14. **Martinac, B., Y. Saimi, and C. Kung.** 2008. Ion channels in microbes. Physiol. Rev. **88:**1449–1490.
15. **McCaig, C. D., A. M. Rajnicek, B. Song, and M. Zhao.** 2005. Controlling cell behavior electrically: current views and future potential. Physiol. Rev. **85:**943–978.
16. **Morini, R., and A. Becchetti.** 2010. Integrin receptors and ligand-gated channels. Adv. Exp. Med. Biol. **674:**95–105.
17. **Mycielska, M. E., and M. B. Djamgoz.** 2004. Cellular mechanisms of direct-current electric field effects: galvanotaxis and metastatic disease. J. Cell Sci. **117:**1631–1639.
18. **Robinson, K. R.** 1985. The responses of cells to electrical fields: a review. J. Cell Biol. **101:**2023–2027.
19. **Sato, M. J., et al.** 2009. Switching direction in electric-signal-induced cell migration by cyclic GMP and phosphatidylinositol signaling. Proc. Natl. Acad. Sci. U. S. A. **106:**6667–6672.
20. **Shanley, L. J., P. Walczysko, M. Bain, D. J. MacEwan, and M. Zhao.** 2006. Influx of extracellular $Ca2^+$ is necessary for electrotaxis in *Dictyostelium*. J. Cell Sci. **119:**4741–4748.
21. **Song, B., et al.** 2007. Application of direct current electric fields to cells and tissues in vitro and modulation of wound electric field in vivo. Nat. Protoc. **2:**1479–1489.
22. **Swaney, K. F., C. H. Huang, and P. N. Devreotes.** 2010. Eukaryotic chemotaxis: a network of signaling pathways controls motility, directional sensing, and polarity. Annu. Rev. Biophys. **39:**265–289.
23. **Uysal-Onganer, P., and M. B. Djamgoz.** 2007. Epidermal growth factor potentiates in vitro metastatic behaviour of human prostate cancer PC-3M cells: involvement of voltage-gated sodium channel. Mol. Cancer **6:**76.
24. **Van Duijn, B., and S. A. Vogelzang.** 1989. The membrane potential of the cellular slime mold *Dictyostelium discoideum* is mainly generated by an electrogenic proton pump. Biochim. Biophys. Acta **983:**186–192.
25. **Van Duijn, B., S. A. Vogelzang, D. L. Ypey, L. G. Van der Molen, and P. J. Van Haastert.** 1990. Normal chemotaxis in *Dictyostelium discoideum* cells with a depolarized plasma membrane potential. J. Cell Sci. **95:**177–183.
26. **Van Duijn, B., D. L. Ypey, and L. G. Van der Molen.** 1988. Electrophysiological properties of *Dictyostelium* derived from membrane potential measurements with microelectrodes. J. Membr. Biol. **106:**123–134.
27. **von der Mark, K., J. Park, S. Bauer, and P. Schmuki.** 2010. Nanoscale engineering of biomimetic surfaces: cues from the extracellular matrix. Cell Tissue Res. **339:**131–153.
28. **Zhao, M., A. Agius-Fernandez, J. V. Forrester, and C. D. McCaig.** 1996. Directed migration of corneal epithelial sheets in physiological electric fields. Invest. Ophthalmol. Vis Sci. **37:**2548–2558.
29. **Zhao, M., T. Jin, C. D. McCaig, J. V. Forrester, and P. N. Devreotes.** 2002. Genetic analysis of the role of G protein-coupled receptor signaling in electrotaxis. J. Cell Biol. **157:**921–927.